RESEARCH ON FLUID HEAT TRANSFER CHARACTERISTICS OF HEAT PIPE RADIATOR DIRECTLY DRIVEN BY HEAT PUMP

Jianhui Niu[1,3], Zheng Liang[1], Shuxue Xu[*2],

[1] College of Energy and Environmental Engineering, Hebei University of Architecture, Zhangjiakou 075000, China

[2] College of Environmental and Energy Engineering, Beijing University of Technology, Beijing 100124, China

[3] Hebei Technology Innovation Center of Phase Change Thermal Management of Data Center, Hebei University of Water Resources and Electric Engineering, China

[*] Shuxue Xu; E-mail: xsx@bjut.edu.cn

The heat pipe radiator directly driven by heat pump heating system has the advantages of fast heat transfer and high energy efficiency. Based on the empirical heat transfer formula, the heat and mass transfer process in the heat pipe radiator was studied. The key parameters in the empirical heat transfer formula were derived by combining with the experimental data. The distribution of the thickness of the condensate film and the heat transfer coefficient in the height direction of the heat pipe radiator was analysed. The influence of the working fluid condensate mass and vapour mass in the heat pipe radiator was investigated. The results showed that the thickness of the liquid film changes from the bottom of 0.1110 mm to the top of 0.0594mm along the height of the heat pipe. The minimum charge of working fluid is 1.78 kg to 1.81 kg and the heating COP of the system still reach to 3.14 even at the outdoor temperature of -12.6 ℃.

Keywords: *heat pump; heat pipe radiator; heating performance; heating COP*

1. Introduction

Since 2003, China's Beijing, Tianjin and Hebei region has mainly carried out the "Coal to Electricity" project, replacing the original household small coal-fired boilers with electric driven clean heating equipment. Coal-fired power plants still dominate the electricity market in Southeast Asia, supplying around 30 % of the total demand [1]. Heat pump is an energy-saving device that uses high-level energy to flow heat from low-level heat source to high-level heat source. Its main function is to convert low-level heat energy that cannot be directly used into high-level heat energy that can be used. Heat pump can not only save energy, but also achieve the effect of environmental protection. Because it does not use combustion mode, it can greatly reduce urban air pollution. Ministry of Environmental Protection has been pointed out that in the process of project implementation, the air source heat pump is the mainstream alternative products [2]. Heat pump has the advantages of energy saving, environmental protection and convenience. In 2009, the European Commission issued a renewable energy directive, which defined 'air thermal energy 'as 'energy in ambient air 'and

incorporated it into the category of renewable energy [3]. For the air source heat pump, heat is absorbed from the air and the water is heated to 40~45℃, and then the hot water is dissipated indoors through the heat dissipation end, such as fan coil, radiator, etc. The capacity of main kind domestic room heating air source heat pump are 3HP or 5HP. Actual operation test results show that, the heating COP can reach to 1.8 at outdoor temperature -20℃ and the average heating COP is about 2.2~2.6 at outdoor temperature -12℃.

In the early 1940 s, some scholars put forward the theory of heat pipe. After the 1980 s, the heat pipe technology continued to mature, the cost was reduced, and the heat pipe technology gradually entered different production fields [4]. Heat pipe is an efficient two-phase heat transfer device, which has much better heat transfer performance than conventional heat transfer equipment. The air source heat pump is driven by the air source, and the heat pipe radiator is used as the heat dissipation end, so a new heating device can integrate the advantages of the two equipment. The heat pipe is used at the evaporation end of the heat pump, which can enhance the heat absorption capacity at the low temperature end [5]. Zhang et al applied heat pipe to solar heat exchanger, and the results show that the coefficient of performance is 1.5 ~ 4 times higher than that of traditional heat exchanger [6]. It is used to give full play to the advantages of heat pipe heat uniformity at the condensation end, the comfort degree can be also improved, and it is more suitable for floor heating. Researchers provided heat to the room through the composite floor of heat pipe, they used the low temperature heat pipe wall radiation radiator as the heating end, the indoor heating temperature could be 2-3℃ lower than the convection heating temperature, and the energy saving is about 25% [7-9]. Peng et al. studied and proved the thermal comfort and indoor temperature distribution of the combined system by the method of combining experiment and simulation, but the operation characteristics of the system were not monitored and studied in detail [10].

Condensation heat transfer characterized by phase change is widely used in building air conditioning and electronic equipment cooling. The research of condensation heat transfer mostly focuses on the condensation heat transfer inside the tube and the bead condensation outside the tube [11-13]. The thickness distribution of liquid film is the most important factor affecting the condensation heat transfer. Nusselt (1916) deduced the theoretical analysis solution of film condensation heat transfer on vertical flat wall, and the research on heat transfer of film condensation on outer layer of tube tended to be mature [14]. Nusselt's theoretical model has been well applied in heat transfer analysis of large diameter horizontal smooth tube bundle [15]. Based on the assumption that the steam and liquid flow in the heat pipe is a steady in-compressible laminar flow with constant boundary conditions, a simplified heat pipe model was established. The pressure distribution and theoretical heat transfer limit of the steam and liquid in the heat pipe were predicted. Therefore, a relatively complete heat management theory was proposed for the first time. Jiao et al. established a mathematical model to study the influence of liquid filling rate on the heat transfer characteristics of gravity heat pipe and proposed the range of liquid filling rate to keep the stable and effective operation of gravity heat pipe [16]. Tsai et al. studied the influence of bending angle, liquid filling rate and shape of heat pipe on heat transfer performance [17]. Zhan et al. used numerical simulation method to study the boiling condensation process in gravity heat pipe and the influence of inclination angle and heating power on its heat transfer performance [18]. Solanki et al. studied the condensation heat transfer of R134a in a horizontal tube with annular flow [19]. Qian et al. proposed a composite substrate-heat pipe fin radiator for cooling power devices. The substrate of the radiator has good temperature

uniformity [20]. The results show that the flow resistance and energy loss of vapor will increase if the vapor core thickness is too small. Different structures of wicks mainly affect the steam flow characteristics through the difference in the width of the steam channel. The smaller the vapor core thickness is, the more easily it is affected by the bending radius and bending angle of the bending section [21]. The thermal resistance of the heat pipe decreases with the increase of the liquid filling rate or heating power. In a certain range, the thermal resistance of the heat pipe decreases with the increase of the inner diameter, and increases first and then decreases with the increase of the condensation section length, but the length of the condensation section should not be too small, which will lead to poor gas-liquid circulation [22].

A novel compact heat pipe/heat pump system was introduced in paper [23], the heat pump condenser was directly coupled with the heat pipe radiator, which reduced the charge of the working medium of the heat pump, the heat transfer temperature difference was reduced, and started faster and had better regulation. In another paper [24], the design method of the new system was introduced in detail and an experimental new system was developed. In this paper, the heat transfer mechanism of the heat pump directly driven heat pipe system was analyzed and studied by the method of combining numerical calculation and experimental research. The physical and mathematical models of condensation heat transfer in heat pipe were established, and the heat transfer process was calculated. The distribution law and heat transfer characteristics of condensation film in heat pipe were analyzed. The experimental device of the system was built, and the key parameters in the calculation model were corrected combined with the experimental data. The research is expected to provide a reference for the design of new domestic heating device.

2 Methodology

2.1 System description

Fig. 1. shows the diagram of the heat pipe radiator directly driven by heat pump heating system. The device consists of a compressor with rated power of 1.5HP and four pieces of heat pipe radiators connected in series. The high-temperature and high-pressure refrigerant vapor discharged from the compressor first enters into #1 heat pipe radiator and then #2, #3 and #4 heat pipe radiator in turn, where the heat is released in the condensing tube bundle and transferred to the heat pipe group. The heat is supplied to the room through the heat pipe group. The working fluid of the heat pump completely condenses and becomes liquid with a certain degree of sub-cooling after leaving the radiator.

The working principle of the heat pipe radiator directly driven by heat pump system is as follows: the inside of the heat pipe is pumped into a vacuum state by a vacuum pump, and then the second working medium is charged into it. At the initial moment, the working medium is in the liquid form at the bottom of the lower header; the heat of the heat pump system is transferred to the heat pipe working medium in the lower header through the condensing coil, and when the heat increases the temperature of the working medium to the evaporation temperature, the liquid will evaporate into vapour. At the same time, the steam comes into contact with the bare wall, an adhesive layer is formed. The rapid condensation process makes it form a multi-molecular liquid film and heat is released. The heat is transferred to the room through thermal radiation and convective heat transfer. Then it flows back to the lower header under the action of gravity.

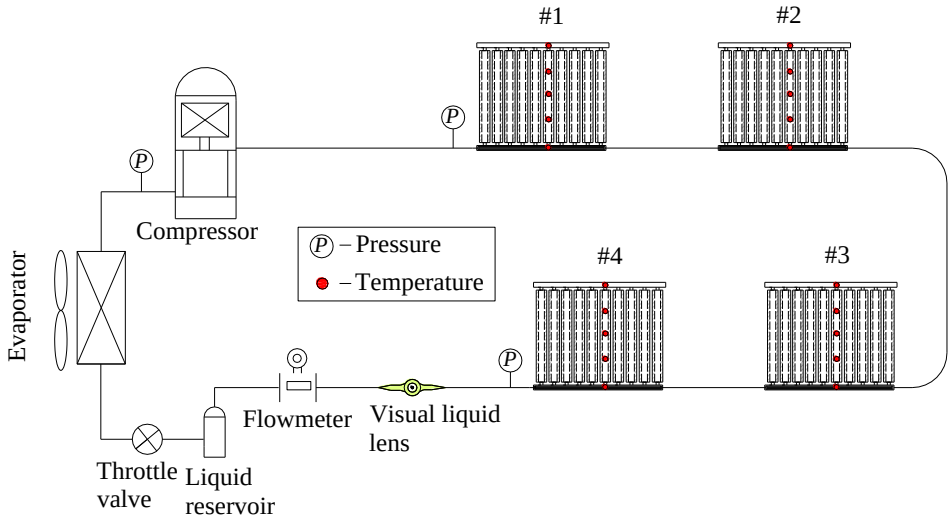

Fig. 1. Heat pipe radiator directly driven by heat pump heating system

The structure parameters of the heat pipe radiator is shown in Fig. 2. (a) and the structure of the lower collection tube is shown in Fig. 2. (b). The heat pump condenser is inserted into the bottom of the heat pipe radiator. The inlet and outlet pipes extend from both sides of the lower header and are isolated and welded as a whole. The condensing tube bundle, as the driving heat source, is immersed in the working medium R134a of the heat pipe. Multiple Heat pipe radiators connected in series can realize the heating of multiple rooms. The structure and quantity of the heat pipe radiator can be flexibly designed, and a single heat pipe radiator can be made with different height and width. The heat pipe radiator in the research has a height of 800 mm and a width of 1310 mm. The condensing tube bundle is of an outer diameter of 9.52 mm and a wall thickness of 2 mm.

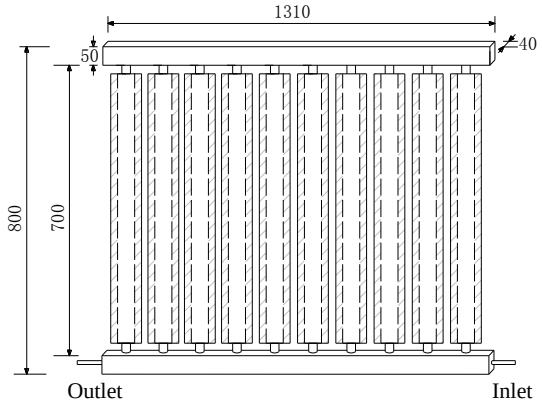

(a)Structure parameters of the heat pipe radiator

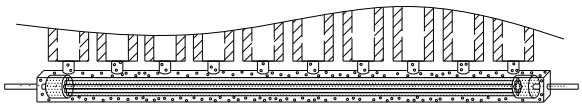

(b) Structure of the lower collection tube

Fig. 2. Heat pipe radiator structure diagram

During operation, the working liquid in the heat pipe evaporates to the inner wall and condenses to form a liquid film after heat dissipation. The thickness of the liquid film is related to the internal

temperature and external temperature. Therefore, the amount of working fluid required to participate in the working cycle must also be related to the working conditions.

2.2 Calculation of heat transfer process of heat pipe

Fig. 3. shows the theoretical model of film condensation. The refrigerant vapour discharged from the compressor of the heat pump enters into the condensing tube bundles, and the heat is dissipated through the heat pipe radiator. The heat transfer in the condenser is mainly latent heat, so the design method aims at the heat transfer calculation of phase change process. Based on that, the shape of the heat pipe radiator and the geometric dimension of the inner tube bundle will be determined.

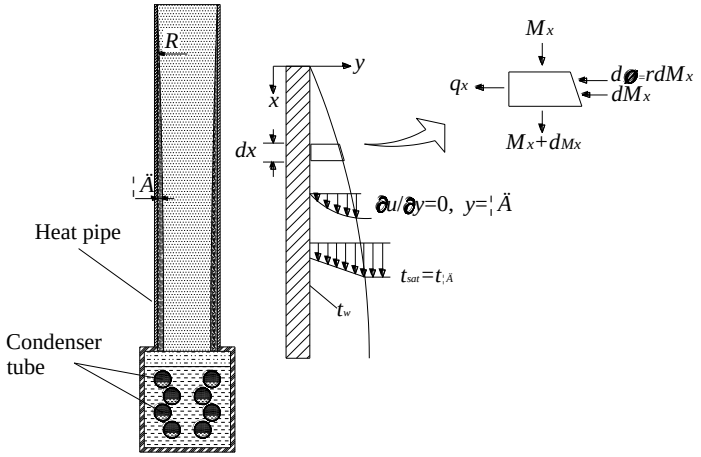

Fig. 3. Theoretical model of film condensation

Based on Nusselt's theory, there are some basic hypothesis [25], which includes:

a. The pure vapor condenses into a laminar liquid film on the wall, and the physical properties are constant.

b. Ignoring shear force and there is no temperature gradient at the vapor liquid film interface, that is $t_\delta = t_{sat}$ as shown in Figure 3.

c. Condensation heat passes through the liquid film in a thermally conductive manner.

d. Ignoring liquid film sub-cooling.

e. Ignoring the thermal resistance of the heat pipe wall, that is $t_w = t_f$.

The momentum equation of condensate film can be simplified as:

$$\frac{\partial^2 u}{\partial y^2} = -\frac{g}{\eta_l}\left(\rho_l - \rho_v\right) \tag{1}$$

Where, u is velocity of the condensate film, m/s; g is gravitational acceleration, m/s^2; η_l is liquid dynamic viscosity, Pa·s; ρ_l is density of saturated liquid, kg/m^3; ρ_v is density of saturated vapour, kg/m^3.

Integral twice and use boundary conditions,

(a)The non-slip boundary conditions at the wall are as follows:

$$y = 0, u = 0, t = t_w \tag{2}$$

Where, t_w is wall temperature of heat pipe, ℃.

(b)Velocity gradient and temperature of gas liquid interface.

$$y = \delta, \frac{\partial \mathrm{u}}{\partial y} = 0, t_\delta = t_{sat} \tag{3}$$

Where, δ is the liquid film thickness, m, t_δ is the liquid film temperature at gas-liquid interface, ℃; t_{sat} is saturated gas temperature, ℃.

Velocity distribution function in condensate film,

$$u(y)=\frac{g(\rho_l-\rho_v)\delta^2}{\eta_l}\left[\frac{y}{\delta}-\frac{1}{2}\left(\frac{y}{\delta}\right)^2\right] \tag{4}$$

Calculation of liquid film velocity on inner wall of heat pipe,

$$u_C=C\frac{g(\rho_l-\rho_v)\delta^2}{\eta_l} \tag{5}$$

Where C is the parameter related to the arrangement of condensing tube bundles.

The condensate flow rate at the position x of the inner wall of the vertical pipe with the inner diameter d is obtained:

$$M_x=\pi d\delta\rho_l u_c=C\frac{\pi dg\rho_l(\rho_l-\rho_v)\delta^3}{\eta_l} \tag{6}$$

Where M_x is condensate flow rate at local position x, kg/s; π is circular constant; d is inner diameter of the heat pipe, m.

The increment of liquid film mass flow rate in the microelement section of d_x is,

$$dM_x=C\frac{3\pi dg\rho_l(\rho_l-\rho_v)^2\delta d}{\eta_l} \tag{7}$$

The latent heat of vaporization released by the condensate is equal to the heat conduction through the liquid film with thickness of δ,

$$rdM_x=C\frac{3r\pi dg\rho_l(\rho_l-\rho_v)\delta^2 d\delta}{\eta_l}=\lambda_l\frac{t_{sat}-t_w}{\delta}\pi ddx \tag{8}$$

Where， r is latent heat, kJ/kg; λ_l is liquid thermal conductivity, W/(m·K).

By integrating the above equation with separated variables, it is noticed that when x = 0, δ = 0, the liquid film thickness at any x position on the pipe wall can be obtained.

$$\delta_x=\left[\frac{4\lambda_l\eta_l(t_{sat}-t_w)x}{3Cg\rho_l(\rho_l-\rho_v)r}\right]^{1/4} \tag{9}$$

The latent heat released at the vapor-liquid interface is transferred to the cold surface by means of heat conduction through the thick δ liquid film:

$$q_x=h_x(t_{sat}-t_w)=\lambda_l\frac{t_{sat}-t_w}{\delta} \tag{10}$$

Where, q_x is heat flux at local position x, as shown is Figure 3.

The local condensation heat transfer coefficient are as follows:

$$h_x=\frac{\lambda_l}{\delta_x} \tag{11}$$

$$h_x=\left[\frac{3Cg\lambda_l^3\rho_l(\rho_l-\rho_v)r}{4\eta_l(t_{sat}-t_w)x}\right]^{1/4} \tag{12}$$

If the condensation temperature difference is constant, the average heat transfer coefficient of the liquid film on the inner wall of the whole heat pipe with height can be obtained as:

$$h=0.943\left[\frac{3Cg\lambda_l^3\rho_l(\rho_l-\rho_v)r}{\eta_l(t_{sat}-t_w)L}\right]^{1/4} \tag{13}$$

Where, λ_l is liquid thermal conductivity, W/(m·K); η_l is liquid dynamic viscosity, Pa·s; t_{sat} is saturated

gas temperature, ℃; t_w is wall temperature of heat pipe, ℃; ρ_l is density of saturated liquid, kg/m3; ρ_v is density of saturated vapour, kg/m^3; r is gasification latent heat, kJ/kg; L is length of tube, m.

The physical parameters in the equations are determined by the arithmetic mean temperature of the boundary layer liquid film, except that the latent heat of vaporization and vapor density are determined by the saturation temperature, $t_m=\left(t_{sat}+t_w\right)/2$.

2.3 Modification of the model

Fig. 4. shows a photo of the whole heat pump system, including the outdoor unit and indoor units. The specifications of the experimental system were listed in Tab. 1. A hermetic-type compressor with a nominal capacity of 1.2 kW designed for R22 was installed, and was driven by a DC variable frequency electric motor, whose frequency varied between 0 Hz～120 Hz. There was one temperature sensor set on the liquid refrigerant tube, which was the position before expansion valve.

(a) Outdoor unit (b) Heat pipe radiators

Fig. 4. Photo of experimental bench

When the compressor was in operation, its speed was controlled by the set value of this temperature point. When the measured value was lower than the set value, the compressor speed increased. When the measured value was higher than the set value, the compressor would continue to run for 3 minutes and then stop.

Tab. 1. Specifications of the new heat pump system

Parameters	Values/details
Compressor	
Compressor type	Rolling piston
Input power (kW)	0-1.5kW
Refrigerant	R22
EEV	
Model	CAREL E^{2}V
Outdoor heat exchanger	
type	Copper tube/aluminum fin
Rated capacity (kW)	4
Number	1
Indoor heat exchanger	
type	Heat pipe
Rated capacity (kW)	1.2
Number	4
Refrigerant	R134a

The parameters to be monitored in the experiment include room temperature t_{room}, outdoor temperature t_{out}, aluminum tube surface temperature t_f, refrigerant mass flow rate of the heat pump M, compressor input power P, *etc*. The sensors locations are shown in Tab. 2.

Tab. 2. Sensors locations of the new heat pump system

Parameters	Location
t_{room}	Room
t_{out}	Outdoor
t_f	Surface of heat pipes
M	Outlet line of heat pipes
P	Compressor input power wire

The total heat transfer capacity of heat pipe radiator is calculated by working fluid flow of heat pump system. Through the experiment of the system, the actual heating capacity of the system can be measured, and then the heating capacity distributed to the single heat pipe radiator can be obtained by the temperature difference method.

$$Q = M\left(h_2 - h_1\right) \tag{14}$$

Where, M is mass flow rate of the heat pump system, kg/s; h_1, $h_2$are inlet and outlet enthalpy of condenser, respectively, kJ/kg.

Heating *COP*:

$$COP = \frac{Q}{p} \tag{15}$$

Where, P is compressor power input (kW).

The uncertainty of indirect measurement data can be obtained by the uncertainty of transfer formula and direct measurement value. If,

$$y = f(x_1, x_2, x_3, \mathrm{L}\ x_n) \tag{16}$$

Therefore, the uncertainty transfer formula of indirect measurement y is as follows [26]:

$$u^2\left(y\right) = (\frac{\partial f}{\partial x_1})u^2\left(x_1\right) + (\frac{\partial f}{\partial x_2})u^2\left(x_2\right) + ... + (\frac{\partial f}{\partial x_n})u^2\left(x_n\right) \tag{17}$$

$$u\left(y\right) = \sqrt{u^2\left(y\right)} \tag{18}$$

The uncertainty of the test results is caused by the measurement errors of the test instruments. According to the accuracy of the selected measuring instruments and the analysis of the uncertainty formula, it can be concluded that the test error of the heating capacity of the test system is 2.1%, and the corresponding test error of the heating *COP* is 3.4%.

Under the condition of indoor temperature, t_{room} was 20 ℃, and outdoor temperature t_{out} was -6 ℃, the experimental results of temperature distribution along the height of heat pipes is shown in Tab.3. From Table 3, it can be seen that the bottom temperature of # 1 and # 2 heat pipes is relatively high, gradually decreasing with height, but increasing again at 800mm. This is due to the influence of the high exhaust temperature in the front section of the heat pump condensation. In the height direction of the heat pipe, the thickness of the condensate film increases, the thermal resistance increases, and the temperature decreases. At the top, due to the thinnest film thickness, the heat transfer is strongest, resulting in an increase in temperature. However, due to # 4 being located at the end of the heat pump, the bottom temperature of # 4 is relatively low. Due to the influence of liquid film thickness, the temperature gradually increases along the height direction. This is also consistent

with the variation law of local surface heat transfer coefficient in Figure 8.

The total heat is equal to the sum of the single heat dissipation of four indoor units, the heat dissipation of a single heat sink is a function of the difference between the surface temperature of heat pipe radiator and the indoor air temperature. The experimental results can be used to fit the empirical formula.

Tab. 3. Temperature distribution along the height of heat pipes

L/mm	#1/℃	#2/℃	#3/℃	#4/℃
0	36.12	35.99	33.40	32.78
200	36.16	35.87	34.84	34.42
400	35.55	35.16	35.00	35.69
600	35.62	35.94	36.84	36.31
800	37.29	36.79	36.82	36.08
C	0.13	0.14	0.13	0.14

$$Q_1 = f(\Delta t_1) = f\left(\overline{t_{f1}} - t_{room}\right);\ Q_2 = f(\Delta t_2) = f\left(\overline{t_{f2}} - t_{room}\right);$$

$$Q_3 = f(\Delta t_3) = f\left(\overline{t_{f3}} - t_{room}\right); Q_4 = f(\Delta t_4) = f\left(\overline{t_{f4}} - t_{room}\right) \quad (19)$$

$$Q = Q_1 + Q_2 + Q_3 + Q_4 \quad (20)$$

Where, $\overline{t_{f1}}$, $\overline{t_{f2}}$, $\overline{t_{f3}}$, $\overline{t_{f4}}$ are average surface temperatures of #1, #2, #3 and #4 heat pipe radiators, respectively,℃; t_{room} is room temperature, ℃; in Fig.5, Δt is average value of Δt_1, Δt_2, Δt_3, Δt_4.

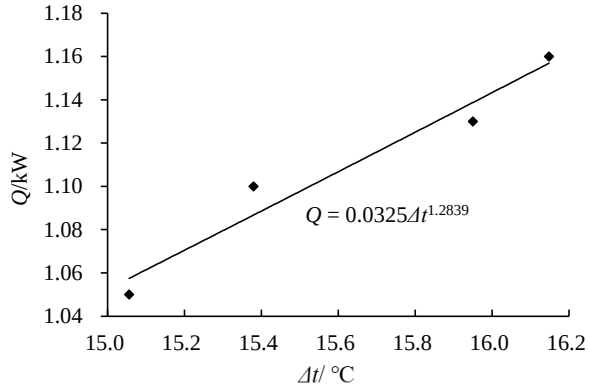

Fig. 5. Relationship between temperature difference Δt and heat dissipation Q

Tab. 4. Comparison of calculated and experimental result

No.	#1	#2	#3	#4
Calculated result, *Q*/kW	1.16	1.13	1.10	1.05
Experimental result, *Q*/kW	1.16	1.14	1.09	1.06
Deviation	0%	+0.88%	-0.91%	+0.95%

As shown in Fig. 5. and Tab. 4, the deviation between the experimental results and the calculated results is less than 1%, and the models intend to match the accuracy of the requirements. Then, the heat dissipation of each heat pipe radiator can be determined according to the surface temperature and room temperature.

Parameter *C* of Eqn (5), which means the empirical parameter of the combination of heating surface and liquid of heat pipe radiator, is determined by the following methods: the heat dissipation of

a single heat pipe radiator, the saturated temperature of R134a in the tube and the wall temperature of the tube are obtained through experiments. Assuming the temperature of the outer wall of the tube, the temperature of the inner wall of the tube is calculated through the heat transfer process equation of the tube wall. Then, according to the temperature value of the inner wall of the tube and the empirical formula of the heat transfer process, the average surface heat transfer coefficient of the condensate film on the inner wall of the tube is calculated. If the error is larger than the experimental value, the temperature of the outer wall of the tube is assumed again until the error of the value meets the requirements. Finally, the value of *C* is determined.

The heating performance of this new heat pump, internal heat transfer and flow of the heat pipes were studied by the method of experiment and theoretical calculation. The system performance mainly adopted the experimental method, and the internal flow process of heat pipes adopted the results of theoretical calculation and experimental results, as shown in Fig. 6.

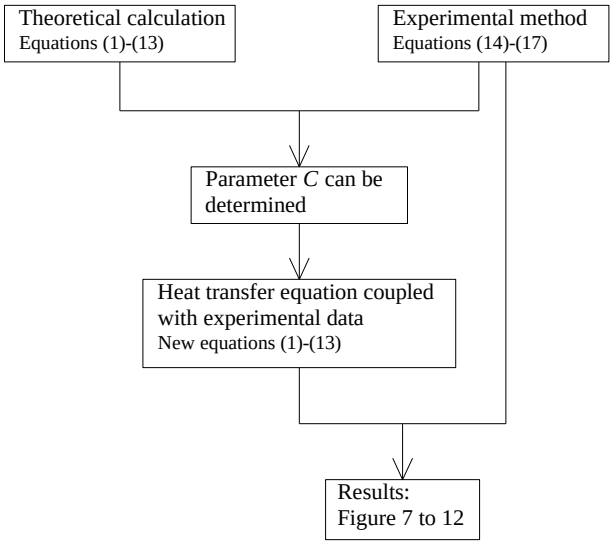

Fig. 6. Relationship between research methods and conclusions

3. Results and analysis

3.1. System performance

The variation of heating capacity, *Q* and heating *COP* under different outdoor temperature is shown in Fig. 7. It can be seen from Figure 6 that at the outdoor temperature of -12.6 ℃, the heating *COP* could still reach to 3.14; at the outdoor temperature of 6.2 ℃, the heating *COP* could reach to 6.30. The energy efficiency coefficient of the system is quite high. The main reason is that the use of heat pipe with high heat transfer coefficient reduces the temperate difference between the condensation temperature of the heat pump and the ambient temperature greatly.

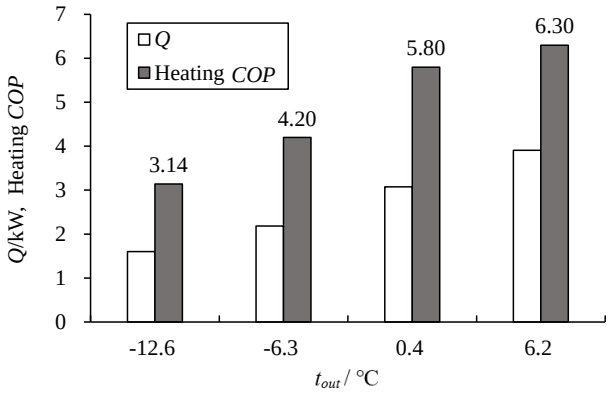

Fig. 7. Heating performance under different outdoor temperature

3.2. Heat transfer and flow characteristics of internal medium

The variation of local liquid film thickness and local heat transfer coefficient with heat pipe height is shown in Fig. 8. The indoor temperature, t_{room} was 20 ℃, and outdoor temperature t_{out} was -6℃. It could be seen that the thickness of the local liquid film, δ_x on the inner wall of the heat pipe decreased with the increase of the heat pipe height, and the local heat transfer coefficient, h_x increased with the increase of heat pipe height. From Figure 8 we can see that when the heat pipe height is 0.4 m, δ_x is 0.1026mm and h_x is 763.29 W/(m^2·K); when the heat pipe height is 0.8 m and 1.2 m, δ_x is 0.0914mm and 0.0730mm, h_x is 851.2 W/(m^2·K) and 1049.18 W/(m^2·K), respectively. When the heat pipe height reaches 1.4 m, the top of the heat pipe , δ_x is only 0.0594 mm, however h_x reaches up to 1268.72 W/(m^2·K).The reason is that, when the gas in the heat pipe contacted with the inner surface of the pipe, it condenses into liquid, and the thickness of the liquid film is gradually superimposed with the decrease of the height, so that the closer to the lower header, the bigger the thickness of the liquid film. The bigger the thickness of the liquid film, the bigger the heat transfer resistance between the steam and the inner wall of the tube was.

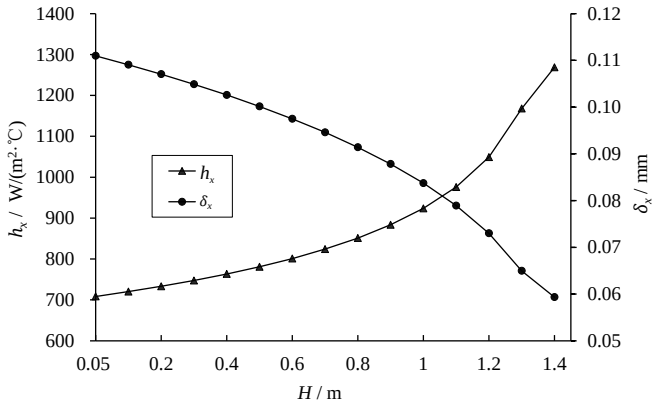

Fig. 8. Variation of local liquid film thickness and local heat transfer coefficient with height

The variation of average liquid film thickness, δ and average heat transfer coefficient, h with indoor temperature is shown in Fig. 9. It could be seen that the average thickness of the liquid film on the inner wall of the heat pipe decreased with the increase of the indoor temperature, and the average heat transfer coefficient increased with the increase of the indoor temperature. From Figure 9 we can see that when the indoor temperature t_{room} is 18 ℃， δ is 0.1068 mm and h is 699.36 W/(m^2·K); when t_{room} is 20 ℃ and 22 ℃， δ is 0.1009 mm and 0.0938 mm, h is 736.03 W/(m^2·K) and 787.17 W/(m^2·K).

when the indoor temperature t_{room} is 26 ℃, δ is only 0.0712 mm and h is 1024.99 W/(m^2·K).The reason is that with the gradual increase of the indoor temperature, the surface temperature of the heat pipe radiator increased, and the evaporation condensation mass flow rate of the working medium in the heat pipe radiator increased, which led to the increase of the downward flow velocity of the condensate film, thus increased the thickness of the liquid film and the heat transfer coefficient increased.

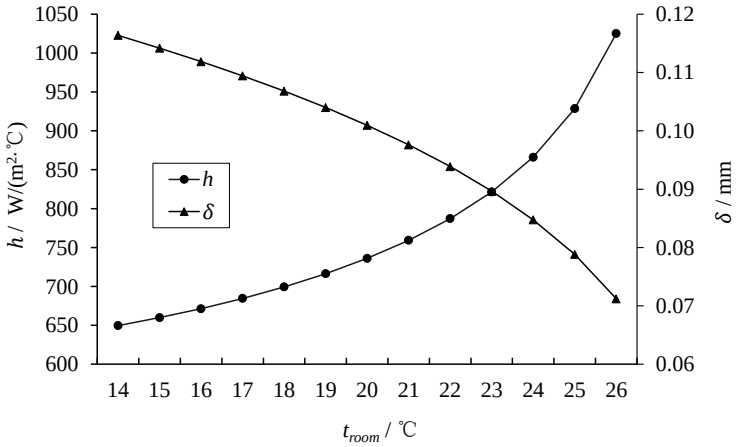

Fig. 9. Variation of average liquid film thickness and average heat transfer coefficient with indoor temperature

As the system working, the working fluid adheres to the inner wall of the heat pipe, its charging amount would affect the heat exchange performance. Thus, the calculation of working medium flow and working fluid charge amount in the heat pipe is very important. Fig. 10. shows the variation of working fluid R134a mass distribution with heat pipe height with indoor temperature 20 ℃ and outdoor temperature -6 ℃. The gas mass is m_g, the liquid mass is m_l. With the increase of the height of heat pipe radiator, the gas-liquid mass ratio of the working fluid decreased gradually, and the variation gradient decreased gradually. When the heat pipe height is 0.8 m, the gas mass m_g is 0.202 kg, the liquid mass m_l is 0.071 kg and the gas-liquid mass ratio m_g/m_l is 2.86. When the heat pipe height is 1.0 m, m_g is 0.353 kg, m_l is 0.093 kg and the gas-liquid mass ratio m_g/m_l is 2.72; when the heat pipe height is 1.4 m, m_g is 0.354 kg, m_l is 0.141 kg and the gas-liquid mass ratio m_g/m_l is 2.52. This is because the heat source was at the lower header of the heat pipe radiator, the evaporated vapour moved upward from the bottom end of the heat pipe, continuously condensed along the inner wall of the heat pipe, and then flowed downward along the wall under the action of gravity. With the condensation process of the steam, the thickness of the liquid film gradually increased, and the proportion of the condensate mass increased gradually. The gas-liquid mass ratio of working fluid increased linearly with the increase of heat pipe height.

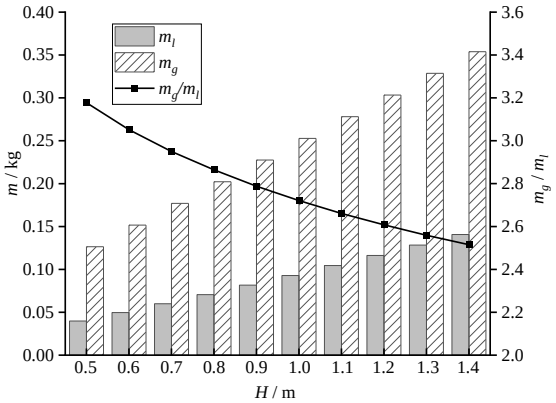

Fig. 10. Variation of working fluid mass distribution with height

Fig. 11. shows the variation of working fluid mass distribution with heat pipe internal diameter with indoor temperature 20 ℃ and outdoor temperature -6 ℃. With the increase of the heat pipe internal diameter, the gas-liquid mass ratio of the working fluid increased gradually. When the heat pipe internal diameter is 0.22 mm, the gas mass m_g is 0.1566 kg, the liquid mass m_l is 0.0622 kg and the gas-liquid mass ratio m_g / m_l is 2.52. when the heat pipe internal diameter is 0.30 mm, m_g is 0.2912 kg, m_l is 0.0848 kg and the gas-liquid mass ratio m_g / m_l is 3.43. when the heat pipe internal diameter is 0.46 mm, m_g is 06846 kg, m_l is 0.1300 kg and the gas-liquid mass ratio m_g / m_l reaches up to 5.27. That is because the heat source was located at the lower header of the heat pipe radiator, the evaporated vapour moved upward from the bottom end of the heat pipe, continuously condensed along the inner wall of the heat pipe, and then flowed downward along the wall under the action of gravity. With the continuous condensation of the vapor, the thickness of the liquid film increased gradually, and the proportion of the condensate mass increased, too. The gas-liquid mass ratio of working fluid increased linearly with the increase of inner diameter of heat pipe.

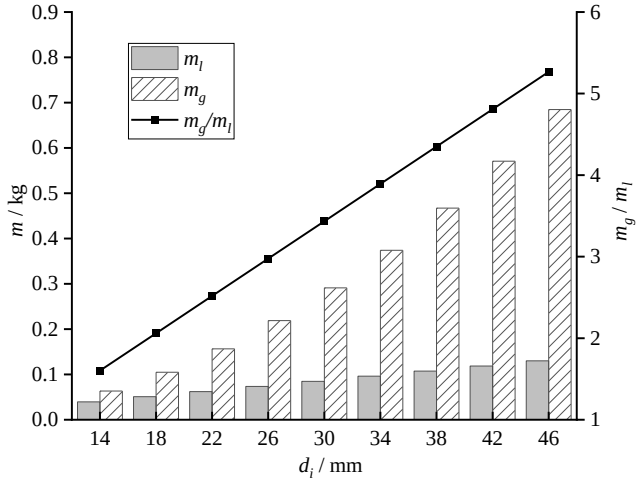

Fig. 11. Variation of working fluid mass with heat pipe internal diameter

4. Discussion

The coil of the condenser was immersed in the working fluid of the lower header of the heat pipe, the heat was transferred through evaporation. The filling amount of heat pipe working fluid should not be too much, within the working condition, it was only to ensure that the condensing coil was always immersed in the working fluid of the heat pipe.

Fig. 12. shows the variation of the minimum charge of working fluid with room temperature under the condition of outdoor temperature -6 ℃.The minimum filling quantity of working fluid was the sum of the working fluid mass in the lower header of radiator, the condensate film mass and the vapor mass on the inner wall of radiator. The minimum charge of working fluid decreased with the increase of room temperature, for this system shown as Fig. 12. it should be 1.78 kg to 1.81 kg. The reason was as follows: the minimum filling quantity of working medium in heat pipe radiator was mainly affected by the condensate quality. With the increase of heating capacity, the room temperature increased, and the mass flow rate of the working fluid evaporation condensation in the heat pipe radiator increased, which led to the increase of the downward flow velocity of the condensate film. Thus, the thickness of the film decreased and the mass of the condensate decreased.

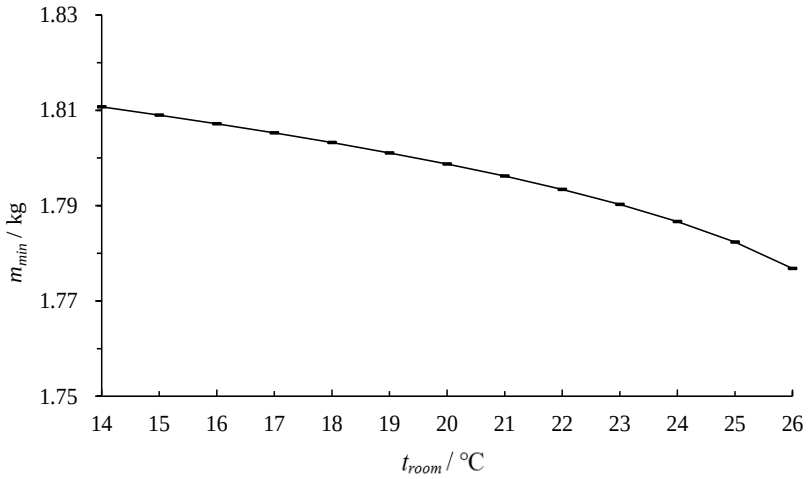

Fig. 12. Variation of minimum refrigerant charge with room temperature

Filling ratio of the working fluid has a predominant effect on the heat transfer characteristics of a two-phase closed heat pipes. A comprehensive model is developed to investigate the effect of filling ratio on the steady-state heat transfer performance of a vertical heat pipe radiator. Compared with other numerical simulations and theoretical calculations of heat transfer in heat pipes, the heat transfer laws are basically consistent [27-28].

5. Conclusions

In this paper, the evaporation and condensation heat transfer process in heat pipe radiator is studied, and the key parameters in the empirical heat transfer formula are derived based on the experimental data. The distribution of condensate film thickness and heat transfer coefficient in height direction in heat pipe radiator is analysed and finally the minimum filling quantity of working fluid was gained.

1) The thickness of the liquid film gradually accumulates along the height direction of the heat pipe, it changes from the bottom of 0.1110 mm to the top of 0.0594mm. The influence of indoor temperature on the heat transfer of the working fluid in the condensation process from gas to liquid also changes from the bottom of 649.59 W/(m^2·K) to the top of 1024.99 W/(m^2·K).

2) With the increase of the height of the heat pipe radiator, the gas-liquid mass ratio of the working fluid decreases from 4.7 to 2.52, and the variation gradient becomes smaller; with the increase of the inner diameter of the heat pipe, the gas-liquid mass ratio increases linearly from 1.60 to 5.27. From the perspective of economy, the diameter of heat pipe can be further reduced and the height of heat pipe can be increased without affecting the indoor heat dissipation.

3) The minimum charge of working fluid decreases with the increase of room temperature. In this research, it was predicted to be 1.78 kg to 1.81 kg. The newly type of heat pump even at the outdoor temperature of -12.6 ℃, the heating COP could still reach to 3.14.

Acknowledgements

This project was funded by Science and Technology Project of Hebei Education Department (Grant No. ZD2022116), Hebei Provincial Graduate Student Innovation Ability Training Project (Grant No. CXZZSS2023161), the Open Project Program of the Hebei Technology Innovation Center of Phase Change Thermal Management of Data Center (Grant No.SKF-2022-08).

Declaration of Interest Statement

The authors declare that they have no known competing financial interests or personal relationships that could have appeared to influence the work reported in this paper.

Nomenclature

C	- parameter related to the arrangement of condensing tube bundles	t	- temperature, [℃]
C_{pl}	- R134a specific constant pressure heat capacity, [kJ/(kg·K)]	t_f	- heat pipes surface temperature, [℃]
h	- average condensation heat transfer coefficient, [W/(m^2·K)]	t_k	- condensation temperature of heat pump, [℃]
h_x	- local condensation heat transfer coefficient, [W/(m^2·K)]	t_{sat}	- R134a saturation temperature, [℃]
h_1	- inlet enthalpy of condenser, [kJ/kg]	t_{out}	- outdoor temperature, [℃]
h_2	- outlet enthalpy of condenser, [kJ/kg]	t_{room}	- room temperature, [℃]
L	- length of tube, [m]	t_w	- wall temperature of heat pipe, [℃]
M	- refrigerant mass flow rate of the heat pump, [kg/s]	u	- velocity, [m/s]
M_x	- condensate flow rate at the position x of the inner wall of the vertical pipe, [kg/s]	*Greeck letter*	
m	- mass, [kg]	δ	- average liquid film thickness, [mm]
m_g	- gas mass, [kg]	δ_x	- local liquid film thickness, [mm]
m_l	- liquid mass, [kg]	η_l	- liquid viscosity of R134a, [Pa·s]
m_{min}	- minimum charge of working fluid, [kg]	λ	- thermal conductivity of aluminium tube, [W/(m·K)]
n	- number	λ_l	- liquid thermal conductivity of R134a, [W/(m·K)]
P	- compressor power input, [kW]	ρ_l	- liquid density of R134a, [kg/m^3]
P_{rl}	- Prandtl number of R134a saturated liquid	ρ_v	- density of R134a saturated gas, [kg/m^3]
Q	- heating capacity, [kW]	σ	- R134a surface tension of liquid steam interface, [N/m]
r	- gasification latent heat of R134a, [kJ/kg]	*Acronyms*	
s	- empirical index	*COP*	- coefficient of performance

References

References

[1]Darmansyah, D., et al., Advancements of Coal Fly Ash and its Prospective Implications for Sustainable Materials in Southeast Asian Countries: A Review[J]. *Renewable and Sustainable Energy*

Reviews, 188(2023).

[2]Ministry of Environmental Protection, National Development and Reform Commission, Ministry of Industry and Information Technology, Ministry of Finance, National Energy Administration. Implementation Rules for the Implementation of the Air Pollution Prevention and Control Action Plan in Beijing, Tianjin and Hebei and the surrounding areas, *104*(2013).

[3]European Commission. 2009 Directive 2009/28/EC on the Promotion of the Use of Energy From Renewable Sources[Z].

[4]Ni, B., et al., Study on Heat Transfer Performance of Pulsating Heat Pipe Heat Exchanger. *Nonferrous Metallurgical Equipment, 37*(2023), 4, PP, 41-47.

[5]Chotivisarut, N., et al., Seasonal Cooling Load Reduction of Building by Thermosyphon Heat Pipe Radiator in Different Climate Areas. *Renewable energy, 38*(2012), 1, PP, 188-194.

[6]Zhang, X.X., et al., Dynamic Performance of a Novel Solar Photovoltaic /Loop Heat Pipe Heat Pump System[J]. *Applied Energy, 114*(2014), 2, PP, 335-352.

[7]Sebarchievici, C., et al., Performance Assessment of a Ground-coupled Heat Pump for an Office Room Heating Using Radiator or Radiant Floor Heating Systems. *Procedia Engineering, 118*(2015), PP, 88-100.

[8]Zhao, W., Zhang. Y.F., Experimental Research on Performance of Low-temperature Thermosyphon Radiant Floor Heating. *Gas & heat, 31* (2021), 7, PP, 26-30.

[9]Jiang, A.H., Fu, J.P., Application of the Low-temperature Heat Pipe Panel Radiator. *Building Energy & Environment*, (2002), 5, PP, 63-64.

[10]Peng, W.J., et al., Experimental and Simulation Study on Thermal Comfort of Direct Expansion Heat Pump Heating System with Different Heat Dissipation Terminals. *Science Technology and Engineering, 20*(2020), 14, PP, 5764 -5771.

[11]Hirose, M., et al., Development of the General Correlation for Condensation Heat Transfer and Pressure Drop Inside Horizontal 4 mm Small-diameter Smooth and Micro-fin Tubes. *International Journal of Refrigeration, 90*(2018), PP, 238-248

[12]Rajkumar, M.R., et al., Experimental Study of Condensation Heat Transfer on Hydrophobic Vertical Tube. *International Journal of Heat and Mass Transfer, 120*(2018), PP, 305-315.

[13]Kim, K., et al., Dropwise Condensation Induced on Chromium Ion Implanted Aluminum Surface. *Nuclear Engineering and Technology, 51*(2019), 1, PP, 84-94.

[14]Lim, H., et al., Energy Saving Potentials from the Application of Heat Pipes on Geothermal Heat Pump System. *Applied Thermal Engineering, 126*(2017), PP, 1191-1198.

[15]Ma, Y.X., et al., Experimental Study on Heat Transfer Performance of Finned Gravity Heat Pipe. *CIESC Journal, 71*(2020), 2, PP, 594-601.

[16]Jiao, B., et al., Investigation on the Effect of Filling Ratio on the Steady-state Heat Transfer Performance of a Vertical Two-phase Closed Thermosyphon. *Applied Thermal Engineering, 28*(2008), PP, 1417-1426.

[17]Tsai, T.E., et al., Dynamic Test Method for Determining the Thermal Performances of Heat Pipes. *International Journal of Heat and Mass Transfer, 53*(2010), 21, PP, 4567-4578.

[18]Zhan, H.R., et al., Simulation Study on Flow and Heat-transfer Characteristics of Gravity Heat Pipes. *Journal of Chinese Society of Power Engineering, 37*(2017), 7, PP, 540-545.

[19]Solanki, A. K., Kumar, R., Condensation Heat Transfer and Pressure Drop Characteristics of R-134a Inside the Flattened Tubes at High Mass Flux and Different Saturation Temperature. *Experimental Heat Transfer, 32*(2019), 7, PP, 69-84(16).

[20]Qian, J.J., et al. Study on Natural Convection Heat Transfer Characteristics of Composite Substrate /Heat Pipe Fin Heat Sink[J]. *Cryogenics & Superconductivity, 51*(2023), 08, PP, 53-59.

[21]Shi, F.Z., Gan. Y.H., Numerical Simulation of Start-up Characteristics and Heat Transfer Performance of Ultra-thin Heat Pipe [J]. *CIESC Journal, 74*(2023), 7, PP, 2814-2823.

[22]Jin, L.Q., et al., Study on the Influence Parameters of Two-phase Heat Transfer Characteristics of Gravity Heat Pipe [J]. *Chinese Journal of Turbomachinery, 65*(2023), 5, PP, 52-57.

[23]Xu, S.X., et al., Investigation of Air-source Heat Pump Using Heat Pipes as Heat Radiator. *International Journal of Refrigeration, 90*(2018), PP, 91-98.

[24]Xu, S.X., et al., Air Source Heat Pump /Heat Pipe Domestic Room Heating System: Design and Experimental Research. *Applied Thermal Engineering, 192*(2021), PP, 116930.

[25]Wang, B.X., Engineering Heat and Mass Transfer (Second Volume), *Beijing: Science Press*, (2020), PP, 451-452.

[26]Moffat, R.J. Using Uncertainty Analysis in the Planning of an Experiment. *Journal of Fluids Engineering, 107*(1985), 2, PP, 173-178.

[27] Zhan, B.R., et al., Simulation Study on Flow and Heat-transfer Characteristics of Gravity Heat Pipes. *Journal of Chinese Society of Power Engineering,37*(2017),7, PP, 540-545.

[28] Jiao, B., et al., Investigation on the effect of filling ratio on the steady-state heat transfer performance of a vertical two-phase closed thermosyphon. *Applied Thermal Engineering, 28* (2008), 1417-1426.

Paper submitted: 07.11.2023
Paper revised: 28.12.2023
Paper accepted: 04.01.2024